

Nano-plasmonics sensing and integration with microfluidics for a lab-on-chip biosensor

By: [Jianjun Wei](#), Matthew Kofke, Megan Rexius, Sameer Singhal, Yi Wang, and David H. Waldeck

J. Wei, M. Rexius, M. Kofke, Y. Wang, S. Singhal, D. H. Waldeck, Nano-plasmonics sensing and integration with microfluidics for a lab-on-chip biosensor, *NSTI-Nanotech 2011* **2011**, 3, 79-82

Made available courtesy of TechConnect Briefs:

<https://briefs.techconnect.org/papers/nano-plamsonics-sensing-and-integration-with-microfluidics-for-a-lab-on-chip-biosensor/>

Abstract:

Ordered arrays of nanostructures in metal films have been studied for practical miniaturization of SPR sensing and microfluidic integration. We report a nanostructure array that is designed to permit significantly enhanced Extraordinary Optical Transmission (EOT) with a tunable primary peak in the visible to NIR range, with the spectral shape and light transmission determined by the surface plasmon (SP) manipulation in the embedded metal film. The array structure readily interfaces with microfluidic channels, making it amenable to highly parallel throughput screening in a lab-on-chip device. The sensing platform may offer greater throughput compatibility, enhanced sensitivity of refractive index changes, improved efficacy of analyte transport, significantly increased EOT intensity for favorable signal-to-noise detection, lower cost, and rapid turnaround times; these qualities will benefit biological binding process and species detection studies and have other applications in healthcare and biomedical research. We present our progress on development of such nanostructured arrays that combines the functions of nanofluidics for effective reagent transport and nanoplasmonics for sensing platform. Our results suggest feasible development of a nano-fluidic-plasmonics-based sensing platform that can be readily integrated with microfluidics devices; hence potentially enabling in-parallel, high throughput transmission SPR lab-on-chip sensing technology.

Keywords: biosensor | microfluidics | nanofluidics | optical transmission | protein | surface plasmon resonance

Article:

*****Note: Full text of article below**

Nano-plasmonics Sensing and Integration with Microfluidics for a Lab-on-chip Biosensor

Jianjun Wei^{*}, Matthew Kofke^{**}, Megan Rexius^{*}, Sameer Singhal^{*}, Yi Wang^{*}, David H. Waldeck^{**}

^{*}CFD Research Corporation, Biomedical Technology Branch
215 Wynn Drive, AL 35805, Corresponding J. Wei jjw@cfdrcc.com

^{**}University of Pittsburgh, the Department of Chemistry,
Pittsburgh, PA, USA, Corresponding D. Waldeck dave@pitt.edu

ABSTRACT

Ordered arrays of nanostructures in metal films have been studied for practical miniaturization of surface plasmon resonance (SPR) sensing and microfluidic integration. We report a nanoslit array that is designed to permit Extraordinary Optical Transmission (EOT) with a tunable primary peak in the visible to NIR range, with the spectral shape and light transmission determined by the SP manipulation in the embedded metal film. The array structure readily interfaces with microfluidic channels, making it amenable to a lab-on-chip device.

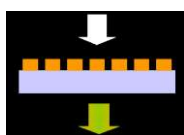
Keywords: nanostructure array, surface plasmon resonance, light transmission, microfluidics, biosensor,

1 INTRODUCTION

While microfluidics has experienced tremendous growth and strongly impacted biomedical research over the past two decades, it remains limited by compatible analysis/detection platforms. In parallel surface plasmon resonance (SPR) methods have shown great flexibility and robustness for detection. Specifically, nanostructured metal films that act as plasmonic sensing elements provide the fundamental technology for a new generation of SPR based assays that are emerging and compatible with microfluidic platforms and/or highly parallel throughput studies.



(a) Kretschmann configuration



(b) Transmission Mode

Figure 1: Two typical SPR configurations

Surface plasmons [1] (SPs) are very sensitive to the near surface dielectric constant (index of refraction) and are well-suited to the detection of surface binding events. Hence they have been exploited extensively in a variety of SPR-based sensors, particular biosensors [2]. The most common methodology of SPR sensing is based on the Kretschmann configuration (Figure 1 (a)) where a prism is used for the light-SP coupling at the surface of a thin metal film. The probe light undergoes total internal reflection on

the inner surface of the prism. At a defined SPR angle, an evanescent light field travels through the thin gold film and excites SPs at the metal-dielectric interface, reducing the intensity of the reflected light. The intensities of scattered and transmitted light fields are used to determine the thickness and/or dielectric constant of the coating [3]. The control variables for SPR sensor applications, i.e., the wavelength of incident light, the thickness of the metal film, the physical and optical properties of the prism and the index of refraction of the medium near the metallic interface, have been well studied [4]. However, the advantages of averaging over a large surface area and challenges of miniaturizing the optics limit the integration of SPR-based sensing with microfluidics [5].

Nanoplasmonics, nano-optical phenomena that are caused by resonant surface plasmons localized in nanosystems, has current and prospective applications in near-field scanning microscopy with chemical resolution, detection of chemical and biological agents with single molecule sensitivity, nano-modification, nanolithography etc. Since Ebbesen et al. [6] demonstrated that an array of subwavelength holes transmits more light than predicted by classical diffraction theory [7] and correlated the extraordinary optical transmission (EOT) to the resonant excitation of surface plasmons that arise from the periodic nature of the arrays [8], nanoscale metal structures have generated considerable interest. On a fundamental level this discovery has sparked interest in the basic process underlying the ability of a nanoaperture to tunnel light with high efficiency and the physics of surface plasmons. On an applied level this work has encouraged researchers to explore the potential for creating nanoscale sensors [9], and other devices from such arrays. Transmission mode SPR (Figure 1 (b)) that is tailored via nanometer scale structures [10] could enable new plasmonic lab-on-chip technologies in bio/chemical sensing. The plasmonic interaction in bio/chemically functionalized nanostructure arrays offers a new strategy for massively parallel detection of chemical and biological agents that bind to functionalized surfaces. Modulation of the nanoaperture array's optical response by adsorbed analytes is expected to offer improved sensitivity and selectivity over conventional SPR methods. In addition, by avoiding use of bulky optics and high-precision mechanics for angular or wavelength interrogation of metal films in contact with analytes [11], it should be possible to

implement and automate the transmission SPR based sensor in compact instrumentation

In this paper, we report the possibility of using a nanoslit array metal film as a biosensor biosensor for a retinol binding protein (RBP) β -Lactoglobulin (β -LG) detection. First, we investigated the correlation between the period of nanoslit and the primary transmission peak position and shape to help selection of the best nanoslit array for protein sensor. Self-assembled monolayers (SAMs) of alkanethiolates on gold provide a convenient way to display a ligand protein on a nanoslit surface with control over the average in-plane density. Additionally, integration of nanoslit arrays to a PDMS microfluidics has been demonstrated as a lab-on-chip device functioning for sample handling and sensing.

2 EXPERIMENTAL SECTION

2.1 Fabrication of Gold Nanoslits

Nanoaperture arrays are fabricated with either a focused ion beam system (FIB) or with E-beam lithography (EBL). FIB is well suited to rapid prototyping while EBL excels at large scale pattern generation. In this work, we fabricated the metallic nanoslit arrays in a two-step process using the standard FIB methodology. Cleaned quartz substrates were placed into an e-beam evaporator (Thermionics VE-180) and Au was evaporated thermally at a pressure of $<10^{-5}$ Torr. A very thin (1-3nm) Ti layer was evaporated first to enhance the adhesion of the Au to the quartz surface. Following thin film evaporation, nanoslits were milled with a focused ion beam system (Seiko 3050SE) at 30kV accelerating voltage with a 30 - 100pA current. For a typical nanoslit array, 40 individual nanoslits were fabricated with a spacing that defined the array's periodicity. For transmission measurements, a reference window was milled into the same Au film that contains no nanoslit arrays. Figure 2 shows two nanoslit structures milled within a 100 nm Au film with a cross section to better view of the nanoslits in the metal film.

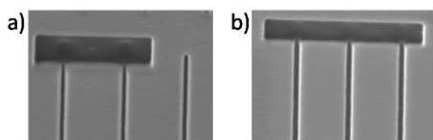


Figure 2: SEM cross section of two FIB milled nanoslit arrays within a 100nm Au film: a) 60nm Slits and b) 120nm Slits. The width of the slit was controlled with the ion beam current used during fabrication

2.2 Preparation Nanoslit Array Biosensor for Protein Detection

Self-assembled monolayer (SAM) and chemical cross-linking reaction were used to modify the gold nanoslit surfaces for biosensor chip preparation. The retinal terminated self-assembled monolayer were prepared by the

follows the procedure. Initially, 1 mM of (1:2 ratio of 8-Hydroxy-1-octanethiol to 11-Amino-1-undecanethiol, Dojindo Molecular Technologies, Inc) alkanethiols in ethanol was prepared for the first mixed alkanethiol SAM with $-NH_2/OH$ terminal moieties. Gold film nanoslit slides were incubated in the solution for 8-12 hours at room temperature. All-trans-retinal (from Sigma) was immobilized covalently to the amino-terminated SAM via formation of a Schiff's base followed by reduction with $NaCNBH_3$ (from Sigma), which is a selective reductant for imines. Finally, excess trans-retinal and reductant were removed at room temperature by extensive washing with methanol and then with acetone, and the washed gold nanoslit surfaces were dried with N_2 gas stream and stored in dark for the next usage.

To ensure the SAM preparation and retinal attachment, water drop contact angles using goniometry were measured after each step preparation. Table 1 presents the typical contact angles for a gold surface, a gold surface after the SAM of $-NH_2/OH$, and after covalently grafting retinal to $-NH_2$. These data demonstrate that different SAM coatings are prepared by the surface modifications, selective binding of β -LG vs. α -LG.

Surface	Au film	NH_2/OH SAM	Retinal SAM	β -LG (0.5 mg/mL)	α -LG (0.5 mg/mL)
Contact angle	64 \pm 3	50 \pm 1	80 \pm 2	46 \pm 2	77 \pm 3

Table 1: static water Contact angles of different surfaces

2.3 Measurements of Transmission Spectra

The EOT through the Au nanoslit array was characterized in the spectral range of 400 nm – 1800 nm, using unpolarized light at normal incidence. Transmission measurements were taken with a fiber coupled spectrometer (QE65000, Ocean Optics, or a CRAIC microspectrophotometer). White light provided by a tungsten/halogen source was coupled into an optical fiber that was collimated and/or focused onto the nanoslit array at normal incidence. The transmitted light was collected with a high NA infinity corrected objective, collimated with the microscope optics, and transmitted to a detector. Transmission data was collected as a percent transmittance or normalized to the area occupied by the nanoslits.

2.4 Microfluidics Integration

Gold nanoslit arrays on micro-gold film pads were fabricated on a glass platform with specifications matching the dimensions as determined by the PDMS microfluidic network. The PDMS network and glass platform were prepared for irreversible bonding by plasma oxidation. PDMS network and nanoslit array alignment was crucial for successful integration. We used a control system for broad and fine adjustments within the field of view of an inverted Nikon microscope's stage. A small micro-control box for fine (micro-scale) x, y and z translational adjustments was

bolted above a large control box capable of broad scale x, y, and z translational adjustments. Precise integration of the glass platform with nanoslit arrays and the microfluidic network was accomplished with our setup. Figure 3 displays the integrated PDMS microfluidics on a quartz substrate where a micro-gold film pads were fabricated and aligned in the microfluidic channels.

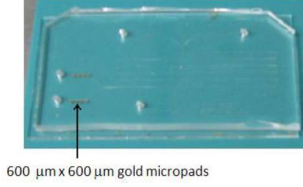


Figure 3: The integrated device with eight gold micropads of 4 in an array: three of them with nanoslit arrays and the other one has a reference window

3 RESULTS AND DISCUSSION

3.1 Correlation of the Transmission Spectra to Nanoslit Array Periods

The wavelength of SPPs excited by Bragg-type scattering over a two dimensional nanoaperture array can be approximately calculated by

$$\lambda_{SPR}(i, j) = a_0(i^2 + j^2)^{\frac{1}{2}} \left(\frac{\epsilon_d \epsilon_m}{\epsilon_d + \epsilon_m} \right)^{\frac{1}{2}} \quad (1)$$

where ϵ_d and ϵ_m are the dielectric function of the dielectric at the metal/dielectric interface and metal dielectric constant, the i, j indices denote particular surface plasmon modes along x and y, and a_0 is the lattice constant (period) for a square array. The plasmon-mediated transmission is several orders of magnitude higher than expected from Bethe's law for the transmission of light through subwavelength apertures. The EOT spectrum is sensitive to the geometric arrangement of the apertures in the array and the values of the dielectric functions at the metal dielectric interface. Thus, the changing dielectric at the interface of a nanoaperture array will cause the wavelength of the transmission peak to shift; a phenomenon that can be used for biological and chemical sensing.

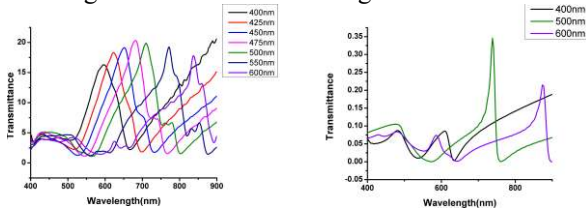


Figure 4: The measured (left) and FDTD simulated (right) transmission spectra for bare Au nanoslit arrays with changing periods

In order to understand the correlation of the transmission spectra to nanoslit array periods, nanoslit arrays with different periodicity ranging from 400 nm -

1000 nm were fabricated using the FIB process. The transmission spectra are presented in Figure 4 (left). We found that there is a single primary resonance which shifts to higher wavelength with increasing period. This is an expected result according to equation 1. The change in shape of the transmission resonance is an interesting result, which is indicative of the complex nature of the transmission process. The transmission SPR modes of the nanoslit arrays periodicities (in air $\epsilon_d = 1$, $\epsilon_m \sim -12$) were calculated by using the finite-difference time-domain (FDTD) method and representative results are shown in Figure 4 (right). In general, the primary transmission peak red shifts and broadens with increasing period. The primary difference between the FDTD spectra and the transmission spectra is the overall width and definition of the peak shape. The experimental transmission peaks are broader and less well defined in general.

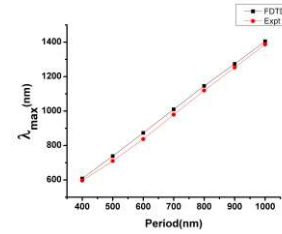


Figure 5: Comparison of λ_{max} from both the FDTD and experimental spectra

The primary transmission peaks (λ_{max}) of different periodicity of the nanoslit arrays from both the FDTD and experimental were extracted and plotted in Figure 5. One can find a linear correlation of the peak red-shift to the nanoslit periodicity. Across all array periods in this work there is good agreement. Both experimental and FDTD transmission spectra show a monotonically increasing value of λ_{max} with the period, but a broad peak width was found for bigger periods.

These results indicate the importance of the period of nanoslit array to determine the transmission peak position as well as the peak width which are important parameters for bio/chemical sensor applications, such as the light source, detector, and sensitivity.

3.2 Nanoslit Array SPR Biosensor for Protein Detection

We demonstrated the use of the nanoslit array of primary transmission peak around 650 nm for a biosensor application in protein detection. A retinol binding protein (RBP), β -Lactoglobulin (β -LG), was selected for this study. As the most abundant whey protein in bovine milk, β -LG plays an important role in the processing of dairy foods, due to its unique structural characteristics, including a buried sulphhydryl group that becomes exposed during thermal denaturation. β -LG has a unique property, which may have physiological significance, of ability to bind small hydrophobic molecules [12], especially retinol. Moreover,

β -LG binds to an immobilized retinal moiety with high affinity [13]. Therefore, taking advantage of this property, we developed a bioselective transmission SPR model sensor for protein detection using the developed metal film nanoslit array with potential use for food quality monitoring by measuring β -LG as a protein ingredient.

The retinal-terminated SAM preparation was accomplished as described in the experimental section. After incubation in a 20 μ g/mL of β -Lactoglobulin (β -LG) in a 20mM pH 5.4 PBS that offers the optimal retention time [14], the nanoslit slide was rinsed by the pH 5.4 PBS and dried under an N_2 stream for EOT spectrum measurement in air.

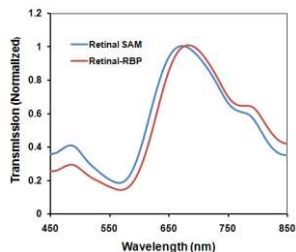


Figure 6: Optical Transmission through an Au Nanoslit Array: Retinal SAM (Blue) and after β -LG Binding (Red).

Figure 6 displays the well-defined EOT spectra of normally incident white light through the nanoslit array after successive surface modification in air. The blue and red curves exhibit all-trans-retinal coated nanoslits and those after the incubation with the retinal binding protein, in the 200 μ g/mL β -LG solution (from bovine milk ~90%, Purchased from Sigma) for 10 min. We found a 10.8 nm peak shift from 672.5nm to 683.3nm after the β -LG binding on the nanoslit; presumably this time is enough to reach binding equilibrium (no extra peak shift with longer incubation time).

The peak shift in the T-SPR shown in Figure 6 is related to changes in the effective dielectric constant at the metallic nanoslit interface due to the protein binding. The effective dielectric constant at the modified interface can be calculated according to reference [4]. Assuming that the nanoslit area is fully covered by the protein β -LG, from the difference of peak shift before and after the protein binding, one can estimate the detection sensitivity of protein β -LG at the retinal SAM in air is 520nm/RIU.

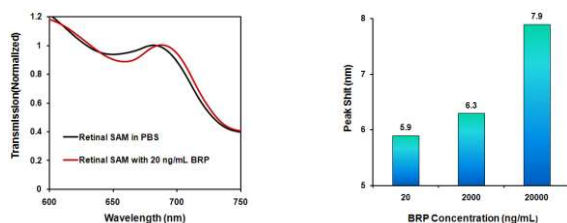


Figure 7: Detection of β -LG in PBS Electrolyte Solution

We also performed the ligand protein detection in aqueous solution. The EOT measurements were performed

in a flow chamber. Various concentrations of β -LG in pH 5.4 PBS were syringed in the chamber into which a nanoslit sensor was sealed and the flow stopped for 5 minutes before collecting the transmission spectra.

Figure 7 shows the transmission spectra in a PBS buffer. The lower intensity of the spectra may result from the background when light transmits through the solution. The sensitivity is estimated to be 3ng/mL (~130 pico-molarity) for protein β -LG at a defined spectral resolution (measurable peak shift resolution is set to 1nm). The results clearly prove that the nanoslit platform, along with tailored surface modification with appropriate receptors, can be used as protein sensors of ultrahigh sensitivity. More work of protein detection in the integrated chip device with a microfluidics system including sample preparation and automated operation are under investigation.

4 CONCLUSION

Transmission spectral properties of nanoslit metal films were investigated with respect to the periods of nanoslit array. Both experimental and FDTD simulation transmission spectra show a monotonically increasing value of λ_{max} with the period, but a broad peak width was found for bigger period. The nanoslit demonstrates ultrasensitive (picomolarity) detection of β -Lactoglobulin in aqueous solution with a modified retinol monolayer nanoslit in a transmission SPR mode. The in-plane nanoslit chip in this study should be compatible to microfluidics and emerging lab-on-chip biosensor application.

ACKNOWLEDGMENT

We thank NASA STTR Program for financial support, and the CFDRB Biomedical Team for their helpful advice and discussions. Additionally we thank Dr. Aaron Weaver from NASA for his technical discussion during this project.

REFERENCES

- [1] H. Raether, Surface Plasmons on Smooth and Rough Surfaces and on Gratings, Springer-Verlag, Berlin Heidelberg, 1988.
- [2] J. Homola, Anal. Bioana. Chem., 377, 528, 2003.
- [3] T. A. Leskova, A. A. Maradudin, and W. Zierau, Opt. Commun. 249, 23, 2005.
- [4] L. S. Jung, C. T. Campbell, T. M. Chinowsky, M. N. Mar, and S. S. Yee, "Langmuir, 14, 5636-5648, 1998.
- [5] I. T. Kim and K.D. Kihm, Exp. Fluids, 41, 905, 2006.
- [6] T. W. Ebbesen, H. J. Lezec, H. F. Ghaemi, T. Thio, and P. A. Wolff, Nature, 391, 667, 1998.
- [7] H. A. Bethe, Phys. Rev. 66, 163, 1944.
- [8] H.F. Ghaemi, T. Thio, D. E. Grupp, T. W. Ebbesen and H. J. Lezec, Phys. Rev. B, 58, 6779, 1998.
- [9] A.G. Brolo, R. Gordon, B. Leathem, and K.L. Kavanagh, Langmuir, 20, 4813, 2004.
- [10] W. L. Barnes, A. Dereux, and T. W. Ebbesen, Nature, 424, 824, 2003.
- [11] W. M. Mullett, E. P. C. Lai, and J. M. Yeung, Methods, 22, 77, 2000.
- [12] G. Kontopidis, C. Holt, and L. Sawyer. J Dairy Sci. 87, 785, 2004.
- [13] H. D. Jang, and H. E. Swaisgood. J. Dairy Sci. 73, 2067 1990.
- [14] Q. Wang, H. E. Swaisgood, J Dairy Sci. 76, 1895, 1993.